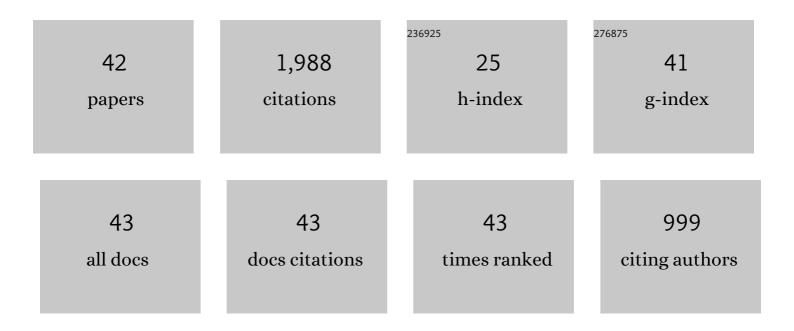
Yu-Qiang Jiang

List of Publications by Year in descending order

Source: https://exaly.com/author-pdf/9751411/publications.pdf Version: 2024-02-01



#	Article	IF	CITATIONS
1	Hot deformation and processing map of a typical Al–Zn–Mg–Cu alloy. Journal of Alloys and Compounds, 2013, 550, 438-445.	5.5	230
2	Hot tensile deformation behaviors and fracture characteristics of a typical Ni-based superalloy. Materials & Design, 2014, 55, 949-957.	5.1	154
3	Hot tensile deformation behaviors and constitutive model of an Al–Zn–Mg–Cu alloy. Materials & Design, 2014, 59, 141-150.	5.1	133
4	Precipitation hardening of 2024-T3 aluminum alloy during creep aging. Materials Science & Engineering A: Structural Materials: Properties, Microstructure and Processing, 2013, 565, 420-429.	5.6	128
5	Hot compressive deformation behavior of 7075 Al alloy under elevated temperature. Journal of Materials Science, 2012, 47, 1306-1318.	3.7	103
6	Effect of creep-aging on precipitates of 7075 aluminum alloy. Materials Science & Engineering A: Structural Materials: Properties, Microstructure and Processing, 2013, 588, 347-356.	5.6	83
7	A Phenomenological Constitutive Model for Describing Thermo-Viscoplastic Behavior of Al-Zn-Mg-Cu Alloy Under Hot Working Condition. Experimental Mechanics, 2012, 52, 993-1002.	2.0	69
8	Precipitation in Al–Cu–Mg alloy during creep exposure. Materials Science & Engineering A: Structural Materials: Properties, Microstructure and Processing, 2012, 556, 796-800.	5.6	68
9	Modeling the high-temperature creep behaviors of 7075 and 2124 aluminum alloys by continuum damage mechanics model. Computational Materials Science, 2013, 73, 72-78.	3.0	65
10	A dislocation density-based model and processing maps of Ti-55511 alloy with bimodal microstructures during hot compression in α+β region. Materials Science & Engineering A: Structural Materials: Properties, Microstructure and Processing, 2020, 790, 139692.	5.6	59
11	Isothermal tensile deformation behaviors and fracture mechanism of Ti-5Al-5Mo-5V-1Cr-1Fe alloy in β phase field. Vacuum, 2018, 156, 187-197.	3.5	56
12	Microstructure evolution and a unified constitutive model for a Ti-55511 alloy deformed in β region. Journal of Alloys and Compounds, 2021, 870, 159534.	5.5	54
13	Spheroidization and dynamic recrystallization mechanisms of Ti-55511 alloy with bimodal microstructures during hot compression in α+β region. Materials Science & Engineering A: Structural Materials: Properties, Microstructure and Processing, 2020, 782, 139282.	5.6	53
14	Hot compressive deformation behavior and microstructure evolution of a Ti-55511 alloy with basket-weave microstructures. Vacuum, 2019, 169, 108878.	3.5	50
15	Hot tensile properties, microstructure evolution and fracture mechanisms of Ti-6Al-4V alloy with initial coarse equiaxed phases. Materials Characterization, 2020, 163, 110272.	4.4	50
16	Modeling the creep behavior of 2024-T3 Al alloy. Computational Materials Science, 2013, 67, 243-248.	3.0	48
17	Effect of creep-aging processing on corrosion resistance of an Al–Zn–Mg–Cu alloy. Materials & Design, 2014, 61, 228-238.	5.1	48
18	Effects of two-stage creep-aging on precipitates of an Al–Cu–Mg alloy. Materials Science & Engineering A: Structural Materials: Properties, Microstructure and Processing, 2014, 614, 45-53.	5.6	45

Yu-Qiang Jiang

#	Article	IF	CITATIONS
19	Effects of creep-aging processing on the corrosion resistance and mechanical properties of an Al–Cu–Mg alloy. Materials Science & Engineering A: Structural Materials: Properties, Microstructure and Processing, 2014, 605, 192-202.	5.6	45
20	High-temperature creep behavior of Al–Cu–Mg alloy. Materials Science & Engineering A: Structural Materials: Properties, Microstructure and Processing, 2012, 550, 125-130.	5.6	43
21	Precipitation behaviors and orientation evolution mechanisms of α phases in Ti-55511 titanium alloy during heat treatment and subsequent hot deformation. Materials Characterization, 2020, 167, 110471.	4.4	42
22	Corrosion resistance of a two-stage stress-aged Al–Cu–Mg alloy: Effects of stress-aging temperature. Journal of Alloys and Compounds, 2016, 657, 855-865.	5.5	36
23	Precipitation behavior of a β-quenched Ti-5Al-5Mo-5V-1Cr-1Fe alloy during high-temperature compression. Materials Characterization, 2019, 151, 358-367.	4.4	34
24	Corrosion resistance of a two-stage stress-aged Al–Cu–Mg alloy: Effects of external stress. Journal of Alloys and Compounds, 2016, 661, 221-230.	5.5	31
25	Effects of creep-aging parameters on aging precipitates of a two-stage creep-aged Al–Zn–Mg–Cu alloy under the extra compressive stress. Journal of Alloys and Compounds, 2018, 743, 448-455.	5.5	28
26	A New Creep Constitutive Model for 7075 Aluminum Alloy Under Elevated Temperatures. Journal of Materials Engineering and Performance, 2014, 23, 4350-4357.	2.5	24
27	Effect of shot peening on static and fatigue properties of self-piercing riveting joints. Journal of Materials Research and Technology, 2022, 18, 1070-1080.	5.8	23
28	Physical property and failure mechanism of self-piercing riveting joints between foam metal sandwich composite aluminum plate and aluminum alloy. Journal of Materials Research and Technology, 2022, 17, 139-149.	5.8	22
29	Precipitation of Secondary Phase and Phase Transformation Behavior of a Solutionâ€Treated Ti–6Al–4V Alloy during Highâ€Temperature Aging. Advanced Engineering Materials, 2020, 22, 1901436.	3.5	21
30	Constitutive Model and Processing Maps for a Tiâ€55511 Alloy in β Region. Advanced Engineering Materials, 2020, 22, 1900930.	3.5	20
31	Effects of aging on precipitation behavior and mechanical properties of a tensile deformed Al–Cu alloy. Journal of Alloys and Compounds, 2020, 843, 155975.	5.5	20
32	Creep and Creep-rupture Behavior of 2124-T851 Aluminum Alloy. High Temperature Materials and Processes, 2013, 32, 533-540.	1.4	17
33	Influence of Stressâ€Aging Processing on Precipitates and Mechanical Properties of a 7075 Aluminum Alloy. Advanced Engineering Materials, 2018, 20, 1700583.	3.5	15
34	Dislocation Density–Based Model and Stacked Autoâ€Encoder Model for Tiâ€55511 Alloy with Basketâ€Weave Microstructures Deformed in α + β Region. Advanced Engineering Materials, 2021, 23, 2001307.	3.5	13
35	Ultrasonic bond process for polymer-based anisotropic conductive film joints. Part 2: Application in chip-on-FR4 board assemblies. Polymer Testing, 2011, 30, 449-456.	4.8	12
36	Effect of initial mixed grain microstructure state of deformed Ni-based superalloy on its refinement behavior during two-stage annealing treatment. Materials Characterization, 2021, 176, 111130.	4.4	12

Yu-Qiang Jiang

#	Article	IF	CITATIONS
37	A New Method to Increase the Spheroidization Rate of Lamellar <i>α</i> Microstructure during Hot Deformation of a Ti–6Al–4V Alloy. Advanced Engineering Materials, 2020, 22, 2000447.	3.5	9
38	Modeling the two-stage creep-aging behaviors of an Al-Cu-Mg alloy. Materials Research Express, 2018, 5, 096514.	1.6	7
39	Joining Properties of SPFC440/AA5052 Multi-Material Self-Piercing Riveting Joints. Materials, 2022, 15, 2962.	2.9	7
40	Effect of low-velocity impact on mechanical property and fatigue life of DP590/AA6061 self-piercing riveted joints. Materials Research Express, 2022, 9, 026514.	1.6	6
41	Microstructural Variation and a Physical Mechanism Model for a Ti-55511 Alloy during Double-Stage Hot Deformation with Stepped Strain Rates in the β Region. Materials, 2021, 14, 6371.	2.9	5
42	Effects of stretching processing parameters on the mean elongation ratio and maximum spread ratio of heavy forgings. Journal of Materials Science, 2011, 46, 7536-7544.	3.7	0